OPEN ACCESS

University of BRISTOL

Publisher's PDF, also known as Version of record

Link to published version (if available):
10.1107/S2052520615019678
10.1107/S2052520615019678/bm5077sup1.cif
10.1107/S2052520615019678/bm50771Asup2.hkl
10.1107/S2052520615019678/bm50771Bsup3.hkl
10.1107/S2052520615019678/bm50771Csup4.hkl
10.1107/S2052520615019678/bm50772Asup5.hkl
10.1107/S2052520615019678/bm50772Bsup6.hkl
10.1107/S2052520615019678/bm50773Asup7.hkl
10.1107/S2052520615019678/bm50773Bsup8.hkl
10.1107/S2052520615019678/bm50774Bsup9.hkl
10.1107/S2052520615019678/bm5077sup10.pdf

Link to publication record in Explore Bristol Research

PDF-document

University of Bristol - Explore Bristol Research

Crystal engineering: co-crystals of cinnamic acid derivatives with a pyridyl derivative co-crystallizer

Daniel A. Lorenzo, Sebastian J. K. Forrest and Hazel A. Sparkes*

Department of Chemistry, University of Bristol, Cantock's Close, Bristol BS8 1TS, England. *Correspondence e-mail: hazel.sparkes@bristol.ac.uk

A number of hydrogen-bonded co-crystals, consisting of a cinnamic acid derivative and a pyridyl co-crystallizer, have been synthesized and their properties investigated by X-ray diffraction. Samples were prepared by recrystallization or solvent drop grinding of *trans*-cinnamic acid (1), 4-methylcinnamic acid (2), 4-methoxy cinnamic acid (3) or 3,4-methoxy cinnamic acid (4), with 4,4-dipyridyl (*A*), *iso*-nicotinamide (*B*) or nicotinamide (*C*). The X-ray single-crystal structures of seven novel co-crystals, obtained through recrystallization, are examined and the hydrogen-bonding interactions discussed. Consistent hydrogen-bonding motifs were observed for samples prepared when using 4,4-dipyridyl (*A*) or *iso*-nicotinamide (*B*) as the co-crystallizing agent. Powder X-ray diffraction analysis of the samples prepared by solvent drop grinding suggests the formation of ten co-crystals.

1. Introduction

The formation of co-crystals is of great importance in a wide range of fields, for example optoelectronics (Zhu *et al.*, 2014, 2015), pharmaceuticals (Brittain, 2012; Steed, 2013) and gas storage or separation (Jones *et al.*, 2011), allowing the properties of compounds and structures to be tuned. While much discussion has gone into the precise nature of co-crystals (Aakeröy *et al.*, 2007; Aitipamula *et al.*, 2012), a widely accepted description is that co-crystals consist of two or more neutral components held together by non-covalent interactions, *e.g.* hydrogen bonding. Given that no covalent bonds are formed or broken in the preparation of a co-crystal, the synthetic design process requires an understanding of intermolecular interactions (Allen *et al.*, 1998, 1999), in order to use crystal engineering (Aakeröy, 1997) approaches based on supramolecular synthons (Hemamalini *et al.*, 2014; Moragues-Bartolome *et al.*, 2012; Bučar *et al.*, 2014; Aakeröy *et al.*, 2012). Alongside the preparation of co-crystals through recrystallization, which is limited by the solubility of the components in different solvents (Braga *et al.*, 2013; James *et al.*, 2012), another method for co-crystal preparation is through mechanochemical grinding of the two species (Braga *et al.*, 2013). The advantage of such an approach is that it is generally environmentally friendly, avoiding the use of large amounts of solvent and usually resulting in a singular product (James *et al.*, 2012).

Co-crystals can possess different physical properties to their respective individual components, for example their habit, solubility, melting point and dissolution rate (Brittain, 2012; Elder *et al.*, 2013). Within the pharmaceutical industry a common problem associated with bringing API's (active pharmaceutical ingredients) to market is poor bioavailability. Pharmaceutical co-crystals which consists of at least one
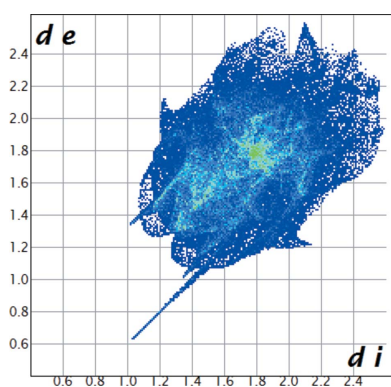
component that is an API can result in a modification of the physiochemical properties, *e.g.* solubility of the API, and thus affect the bioavailability of the species without altering the API's activity (Steed, 2013). Clearly the co-former in the co-crystal needs to be safe for human consumption with no side effects.

The formation of co-crystals between cinnamic acid derivatives and *iso*-nicotinamide has previously been carried out resulting in the formation of 12 co-crystals (Aakeröy *et al.*, 2002). Two distinctive supramolecular hydrogen-bonding motifs were identified in the co-crystals, the first involving the carboxylic acid OH and the N of the pyridyl, and the second amide–amide hydrogen-bonding interactions. In addition one hydrate of 4-hydroxy-3-methoxycinnamic acid and *iso*-nicotinamide has been reported (Clarke *et al.*, 2010); however, this contained amide–carboxylic acid OH···O and NH···O hydrogen bonding rather than amide–amide and carboxylic acid–dipyridyl hydrogen bonding.

Two polymorphic co-crystals of 4-hydroxycinnamic acid (*p*-coumaric acid) and nicotinamide have previously been reported (Bevill *et al.*, 2014). Both of these contain OH···O and NH···O hydrogen bonding between the carboxylic acid and the amide CONH$_2$, with the hydroxyl OH group forming a hydrogen-bonding interaction to the N of the pyridyl group. Two further hydrates of co-crystals containing nicotinamide and a cinnamic acid derivative (3,4-dihydroxy cinnamic acid and 4-hydroxy-3-methoxycinnamic acid; Clarke *et al.*, 2010) also contained OH···O and NH···O hydrogen bonding rather than amide–amide and carboxylic acid–dipyridyl hydrogen bonding.

As part of a wider program of research into the crystalline behaviour of cinnamic acid derivatives (Allen *et al.*, 2005; Howard *et al.*, 2009; Mahon *et al.*, 2008; Yates & Sparkes, 2013), the interaction of four cinnamic acid derivatives [(1)–(4)] with three potential co-crystallizers (*A*)–(*C*) has been investigated in order to obtain further insight into the supramolecular structural motifs formed. Co-crystallizers were selected on their potential to form hydrogen-bonding interactions with the carboxylic acid group (Aakeröy *et al.*, 2002; Seaton, 2011) of the selected cinnamic acids and thus form a co-crystal, see Fig. 1. The results of the preparation of the series of cinnamic acid crystals *via* recrystallization and solvent drop grinding are reported.

2. Experimental

trans-Cinnamic acid (1), 4-methylcinnamic acid (2), 4-methoxycinnamic acid (3), 3,4-methoxycinnamic acid (4), 4,4-dipyridyl (*A*), *iso*-nicotinamide (*B*) and nicotinamide (*C*) along with all solvents were used as received without further purification from Sigma Aldrich.

2.1. General procedure for recrystallization

Small amounts of a cinnamic acid derivative (1)–(4) and a co-crystallizer (*A*)–(*C*) in the appropriate stoichiometric ratio (*i.e.* 2:1 for cinnamic acid:dipyridyl and 1:1 for cinnamic
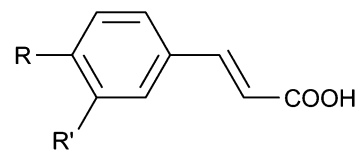
acid:*iso*-nicotinamide and cinnamic acid:nicotinamide) were dissolved in a solvent in which both species were soluble. The vials were left for the solvent to evaporate slowly over a couple of weeks to yield crystals which were analysed by single-crystal X-ray diffraction.

2.2. General procedure for sample preparation by ball milling and solvent drop grinding

Small stoichiometric amounts of a cinnamic acid derivative (1)–(4) and a co-crystallizer (*A*)–(*C*) in the appropriate stoichiometric ratio (*i.e.* 2:1 for cinnamic acid:dipyridyl and 1:1 for cinnamic acid:*iso*-nicotinamide and cinnamic acid:nicotinamide) totalling $\sim$ 0.12 g were loaded into a Retsch MM200 ball mill with $\sim$ 0.04 ml of ethanol. The samples were ground in the ball mill for 30 min at a frequency of 10 Hz. The samples were then analysed using powder X-ray diffraction to check for signs of the formation of a co-crystal.

2.3. Single-crystal X-ray diffraction

Single-crystal X-ray diffraction data collections on (1*A*), (1*B*), (1*C*), (2*A*), (2*B*), (3*A*), (3*B*) and (4*B*) were carried out at 100 K on a Bruker APEXII diffractometer using Mo *Kα* radiation (λ = 0.71073 Å). Data collections were performed using a CCD area detector from a single crystal mounted on a glass fibre. Absorption corrections were based on equivalent reflections using *SADABS* (Bruker, 2001). All of the structures were solved using *SUPERFLIP* (Palatinus & Chapuis, 2007; Palatinus *et al.*, 2012; Palatinus & van der Lee, 2008), and refined against F^2 in *SHELXL* (Sheldrick, 2015) using *OLEX*2 (Dolomanov *et al.*, 2009). All of the O—H or N—H hydrogen atoms were located in the difference map and the majority refined freely; there were a couple of exceptions which required some restraints on the D—H distance and the H atoms attached to the disordered fragment in (2*A*) which were fixed geometrically and refined using a riding model; the

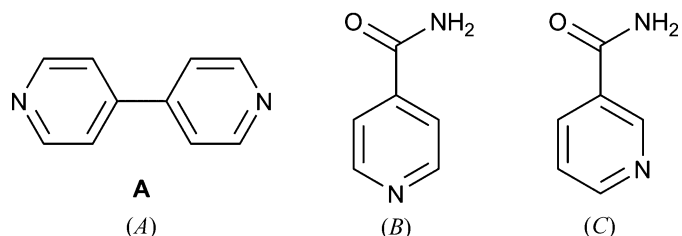(1) R = H, R' = H; (2) R = Me, R' = H; (3) R = OMe, R' = H; (4) R = OMe, R' = OMe

Figure 1
Four cinnamic acid derivatives, *trans*-cinnamic acid (1), 4-methylcinnamic acid (2), 4-methoxy cinnamic acid (3) and 3,4-methoxy cinnamic acid (4). Three co-crystallizers: 4,4-dipyridyl (*A*), iso-nicotinamide (*B*) and nicotinamide (*C*).

Table 1
Experimental details.

	(1A)	(1B)	(1C)	(2A)	(2B)
Crystal data					
Chemical formula	$C_{10}H_8N_2 \cdot 2C_9H_8O_2$	$C_9H_8O_2 \cdot C_6H_6N_2O$	$C_9H_8O_2 \cdot C_6H_6N_2O$	$2C_{10}H_{10}O_2 \cdot C_{10}H_8N_2$	$C_{10}H_{10}O_2 \cdot C_6H_6N_2O$
M_r	452.49	270.28	270.28	480.54	284.31
Crystal system, space group	Monoclinic, $P2_1/n$	Triclinic, $P\bar{1}$	Monoclinic, $P2_1/c$	Triclinic, $P\bar{1}$	Triclinic, $P\bar{1}$
Temperature (K)	100	100	100	100	100
a, b, c (Å)	7.7952 (2), 7.1669 (2), 20.7708 (5)	8.4176 (3), 10.6487 (4), 15.0679 (5)	14.0191 (7), 6.1871 (3), 16.6387 (7)	10.8843 (2), 15.6510 (4), 16.6073 (4)	7.0311 (2), 8.6172 (2), 11.9490 (3)
α, β, γ (°)	90, 93.2075 (17), 90	75.883 (2), 82.329 (2), 83.301 (2)	90, 111.740 (3), 90	63.358 (1), 79.726 (1), 77.722 (1)	77.4101 (14), 87.9565 (14), 82.6358 (14)
V (Å³)	1158.59 (5)	1293.14 (8)	1340.56 (11)	2459.66 (10)	700.71 (3)
Z	2	4	4	4	2
$F(000)$	476	568	568	1016	300
Radiation type	Mo $K\alpha$	Mo $K\alpha$	Mo $K\alpha$	Mo $K\alpha$	Mo $K\alpha$
D_x (Mg m⁻³)	1.297	1.388	1.339	1.298	1.347
μ (mm⁻¹)	0.09	0.10	0.10	0.09	0.09
Crystal size (mm)	$0.63 \times 0.32 \times 0.3$	$0.6 \times 0.47 \times 0.33$	$0.22 \times 0.15 \times 0.13$	$0.67 \times 0.4 \times 0.27$	$0.62 \times 0.35 \times 0.28$
Data collection					
Diffractometer	Bruker APEXII kappa CCD area detector	Bruker APEXII kappa CCDC area detector	Bruker APEXII kappa CCD area detector	Bruker APEXII kappa CCD area detector	Bruker APEXII kappa CCD area detector
Absorption correction	Multi-scan *SADABS* (Bruker, 2001)	Multi-scan *SADABS* (Bruker, 2001)	Multi-scan *SADABS* (Bruker, 2001)	Multi-scan *SADABS* (Bruker, 2001)	Multi-scan *SADABS* (Bruker, 2001)
T_{min}, T_{max}	0.658, 0.746	0.624, 0.746	0.645, 0.746	0.593, 0.746	0.664, 0.746
No. of measured, independent and observed $[I > 2\sigma(I)]$ reflections	10 075, 2759, 2356	11 995, 6048, 4955	11 465, 3188, 2166	45 365, 11 862, 8260	12 831, 3359, 3003
R_{int}, R_{sigma}	0.022, 0.021	0.017, 0.026	0.054, 0.051	0.045, 0.044	0.016, 0.014
$(\sin\theta/\lambda)_{max}$ (Å⁻¹)	0.658	0.660	0.658	0.660	0.658
Refinement					
$R[F^2 > 2\sigma(F^2)], wR(F^2), S$	0.036, 0.095, 1.06	0.039, 0.110, 1.03	0.045, 0.108, 1.00	0.051, 0.138, 1.02	0.035, 0.101, 1.04
No. of reflections	2759	6048	3188	11862	3359
No. of parameters	158	385	193	740	203
No. of restraints	0	0	0	331	0
H-atom treatment	H atoms treated by a mixture of independent and constrained refinement	H atoms treated by a mixture of independent and constrained refinement	H atoms treated by a mixture of independent and constrained refinement	H atoms treated by a mixture of independent and constrained refinement	H atoms treated by a mixture of independent and constrained refinement
$\Delta\rho_{max}, \Delta\rho_{min}$ (e Å⁻³)	0.38, −0.20	0.46, −0.24	0.23, −0.22	0.81, −0.35	0.44, −0.19

	(3A)	(3B)	(4B)
Crystal data			
Chemical formula	$2C_{10}H_{10}O_3 \cdot C_{10}H_8N_2$	$C_{10}H_{10}O_3 \cdot C_6H_6N_2O$	$C_{11}H_{12}O_4 \cdot C_6H_6N_2O$
M_r	512.54	300.31	330.33
Crystal system, space group	Monoclinic, $P2_1/n$	Triclinic, $P\bar{1}$	Monoclinic, $P2_1/c$
Temperature (K)	100	100	100
a, b, c (Å)	6.4681 (3), 28.9773 (13), 6.8930 (3)	9.1225 (4), 11.5523 (4), 14.1938 (5)	14.0200 (8), 9.8795 (5), 11.6434 (6)
α, β, γ (°)	90, 103.812 (2), 90	90.700 (3), 90.577 (3), 104.055 (3)	90, 96.975 (4), 90
V (Å³)	1254.58 (10)	1450.81 (10)	1600.80 (15)
Z	2	4	4
$F(000)$	540	632	696
D_x (Mg m⁻³)	1.357	1.375	1.371
μ (mm⁻¹)	0.10	0.10	0.10
Crystal size (mm)	$0.4 \times 0.35 \times 0.35$	$0.35 \times 0.2 \times 0.13$	$0.37 \times 0.27 \times 0.16$
Data collection			
Diffractometer	Bruker APEXII kappa CCD area detector	Bruker APEXII kappa CCD area detector	Bruker APEXII kappa CCD area detector
Absorption correction	Multi-scan *SADABS* (Bruker, 2001)	Multi-scan *SADABS* (Bruker, 2001)	Multi-scan *SADABS* (Bruker, 2001)
T_{min}, T_{max}	0.637, 0.746	0.560, 0.746	0.672, 0.746
No. of measured, independent and observed $[I > 2\sigma(I)]$ reflections	22 702, 3014, 2677	26 528, 6900, 4151	14 321, 3896, 2262
R_{int}, R_{sigma}	0.032, 0.019	0.070, 0.068	0.085, 0.086
$(\sin\theta/\lambda)_{max}$ (Å⁻¹)	0.661	0.658	0.663

Table 2 (continued)

	(3A)	(3B)	(4B)
Refinement			
$R[F^2 > 2\sigma(F^2)]$, $wR(F^2)$, S	0.041, 0.107, 1.07	0.057, 0.141, 0.99	0.055, 0.134, 1.00
No. of reflections	3014	6900	3896
No. of parameters	177	423	231
No. of restraints	0	1	1
H-atom treatment	H atoms treated by a mixture of independent and constrained refinement	H atoms treated by a mixture of independent and constrained refinement	H atoms treated by a mixture of independent and constrained refinement
$\Delta\rho_{max}$, $\Delta\rho_{min}$ (e Å^{-3})	0.35, −0.25	0.39, −0.32	0.25, −0.32

Table 2
Results of co-crystallization experiments.

Cinnamic acid	Co-crystallizer	Co-crystal formed	Recrystallization	Solvent drop grinding
(1)	(A)	(1A)	Co-crystal formed	Co-crystal formed
(1)	(B)	(1B)	Co-crystal formed	Co-crystal formed
(1)	(C)	(1C)	Co-crystal formed	Co-crystal formed
(2)	(A)	(2A)	Co-crystal formed	Co-crystal formed
(2)	(B)	(2B)	Co-crystal formed	Co-crystal formed
(2)	(C)	(2C)	–	Co-crystal formed
(3)	(A)	(3A)	Co-crystal formed	Co-crystal formed
(3)	(B)	(3B)	Co-crystal formed	Co-crystal formed
(3)	(C)	(3C)	–	Co-crystal formed
(4)	(A)	(4A)	–	Co-crystal formed
(4)	(B)	(4B)	Co-crystal formed	–
(4)	(C)	(4C)	–	–

Table 3
Summary of the hydrogen-bonding parameters (Å, °) in the co-crystals.

	$D-H\cdots A$	$D-H$	$H\cdots A$	$D\cdots A$	$\angle D-H\cdots A$
(1A)	O1—H1A⋯N1	0.96 (2)	1.68 (2)	2.635 (1)	179 (2)
(1B)	O1—H1⋯N1	0.97 (2)	1.67 (2)	2.642 (1)	176 (2)
	O4—H4⋯N3	0.98 (2)	1.65 (2)	2.633 (1)	176 (2)
	N2—H2A⋯O6	0.90 (2)	2.02 (2)	2.911 (1)	176 (2)
	N4—H4B⋯O3	0.89 (2)	2.01 (2)	2.904 (1)	179 (2)
	N2—H2B⋯O5^{i}	0.91 (2)	2.01 (2)	2.908 (1)	171 (2)
	N4—H4C⋯O2^{ii}	0.87 (2)	2.04 (2)	2.906 (1)	171 (2)
(1C)	O1—H1⋯N1	1.00 (3)	1.65 (3)	2.643 (2)	173 (2)
	N2—H2A⋯O2^{iii}	0.94 (2)	1.99 (2)	2.921 (2)	173 (2)
	N2—H2B⋯O3^{iv}	0.91 (2)	1.97 (2)	2.875 (2)	176 (2)
(2A)	O1—H1⋯N2	0.84	1.82	2.63 (2)	161
	O1A—H1AA⋯N2	0.84	1.98	2.79 (1)	164
	O4—H4⋯N4	0.98 (3)	1.69 (3)	2.652 (2)	168 (2)
	O6—H6⋯N3	1.00 (1)	1.66 (1)	2.662 (2)	176 (3)
	O8—H8A⋯N1	0.94 (3)	1.70 (3)	2.635 (2)	173 (2)
(2B)	O2—H2⋯N1	0.97 (2)	1.66 (2)	2.618 (1)	167 (2)
	N2—H2B⋯O1^{v}	0.90 (2)	2.05 (2)	2.939 (1)	170 (1)
	N2—H2C⋯O3^{vi}	0.92 (2)	1.96 (2)	2.880 (1)	174 (1)
(3A)	O1—H1⋯N1	0.95 (2)	1.67 (2)	2.615 (1)	172 (2)
(3B)	O1—H1⋯N3	1.00 (2)	1.66 (2)	2.665 (2)	175 (3)
	O5—H5A⋯N1	1.00 (2)	1.68 (2)	2.675 (2)	173 (2)
	N2—H2A⋯O4^{vii}	0.96 (3)	1.96 (3)	2.917 (2)	173 (2)
	N4—H4A⋯O8^{viii}	0.96 (3)	1.93 (3)	2.878 (2)	175 (2)
	N2—H2B⋯O6^{ix}	0.90 (3)	2.04 (3)	2.934 (2)	173 (2)
	N4—H4B⋯O2^{ix}	0.92 (3)	2.04 (3)	2.953 (2)	171 (2)
(4B)	O1—H1⋯N1	1.000 (1)	1.609 (3)	2.607 (2)	176 (3)
	N2—H2B⋯O5^{x}	0.93 (2)	1.94 (3)	2.869 (3)	176 (2)

Symmetry codes: (i) $1 + x, -1 + y, +z$; (ii) $-1 + x, 1 + y, +z$; (iii) $1 - x, \frac{1}{2} + y, \frac{1}{2} - z$; (iv) $1 - x, 1 - y, -z$; (v) $+x, 1 + y, +z$; (vi) $-1 - x, -1 - y, 1 - z$; (vii) $-x, -y, 2 - z$; (viii) $1 - x, -y, 2 - z$; (ix) $2 - x, 1 - y, 2 - z$; (x) $1 - x, 1 - y, -1 - z$.

C—H hydrogen atoms were located geometrically and refined using a riding model. In the case of (2A) one of the four independent molecules of 4-methylcinnamic acid was disordered, the occupancies of the fragments were determined by refining them against a free variable with the sum of the two sites set to equal 1, the occupancies were then fixed at the refined values, restraints were applied to bond lengths and thermal displacement parameters to maintain sensible geometry in the disordered fragments. Crystal structure and refinement data are given in Table 1.

2.4. Powder X-ray diffraction

Powder X-ray diffraction measurements were carried out on a Bruker D8 Advance powder X-ray diffractometer fitted with a LynxEye detector using Cu radiation (λ = 1.5406 Å). Data collections were made at room temperature, 2θ 5–50°, with a step size of 0.024°. Powder X-ray diffraction measurements were taken from each of the cinnamic acids (1)–(4), the co-crystallizers (A)–(C) and all of the samples from the solvent drop grinding.
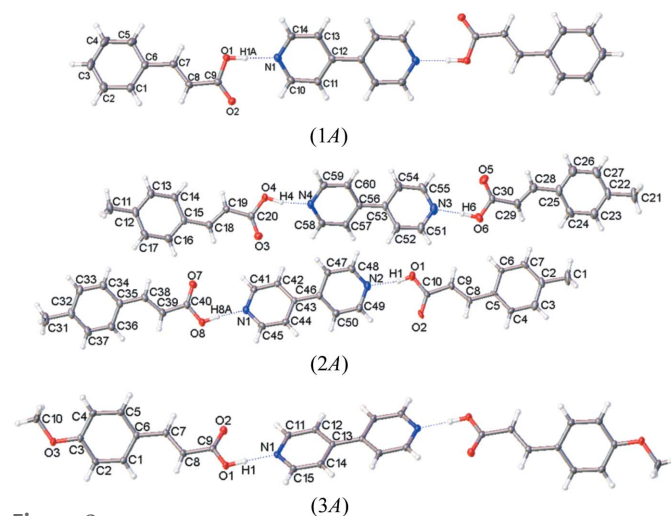

Figure 2
Structure of (1A), (2A) and (3A) with ellipsoids depicted at the 50% level. Hydrogen bonding is illustrated and the atom labelling shown. In structure (2A) only one position of the disordered 4-methylcinnamic acid (C1–C10, O1, O2) is shown.

Table 4
Summary of the π–π contacts in the co-crystals.

	Plane 1	Plane 2	Centroid–centroid distance (Å)	Shift distance (Å)
(1A)	(N1, C10–C14)	(N1, C10–C14)[i]	3.951 (1)	1.970 (2)
(1B)	(C1–C6)	(N3, C25–C29)[i]	3.652 (1)	0.972 (2)
	(C16–C21)	(N3, C25–C29)[ii]	3.700 (1)	0.947 (2)
	(N1, C10–C14)	(N1, C10–C14)[i]	3.868 (1)	1.822 (2)
(1C)	(C1–C6)	(N1, C10–C14)[iii]	3.843 (1)	1.557 (3)
(2A)	(C12–C17)	(N3, C51–C55)[vi]	3.674 (1)	1.010 (2)
	(N3, C51–C55)	(N3, C51–C55)[v]	3.703 (1)	1.411 (3)
	(N1, C41–C45)	(N1, C41–C45)[vi]	3.768 (1)	1.331 (2)
	(N1, C41–C45)	(C2–C7)[vii]	3.683 (1)	1.668 (2)
	(N1, C41–C45)	(C2A–C7A)[vii]	3.652 (1)	1.451 (2)
	(C22–C27)	(C22–C27)[viii]	3.865 (1)	1.615 (3)
(2B)	(C1–C6)	(C1–C6)[ix]	3.984 (1)	1.701 (2)
	(C1–C6)	(N1, C11–C15)[x]	3.825 (1)	1.332 (2)
	(N1, C11–C15)	(N1, C11–C15)[xi]	3.674 (1)	1.592 (2)
(3A)	(N1, C11–C15)	(N1, C11–C15)[xii]	3.754 (1)	1.825 (2)
(4B)	(C1–C6)	(N1, C12–C16)[xiii]	3.900	1.940

Symmetry codes: (i) $2-x, -y, 1-z$; (ii) $-x, 2-y, -z$; (iii) $x, \frac{3}{2}-y, \frac{1}{2}+z$; (iv) $1-x, 1-y, -z$; (v) $1-x, -y, -z$; (vi) $2-x, 1-y, -z$; (vii) $2-x, -y, -z$; (viii) $x, -1+y, -1+z$; (ix) $1-x, 1-y, 2-z$; (x) $1+x, 1+y, +z$; (xi) $-x, -y, 1-z$; (xii) $1-x, 1-y, 1-z$; (xiii) $1+x, +y, 1+z$.

3. Results and discussion

3.1. Recrystallization

Co-crystals were successfully formed from a number of the combinations which are summarized in Table 2. Co-crystals are denoted by a combination of the cinnamic acid number and the co-crystallizer letter, *e.g.* (1A) represents co-crystals of *trans*-cinnamic acid (1) and 4,4′-dipyridyl (A).

3.2. Di-pyridyl (A)

Co-crystals (1A) and (3A) were crystallized from ethanol and THF, respectively. Both structures were obtained in the monoclinic space group $P2_1/n$ with 1 molecule of the cinnamic acid derivative and half a 4,4-dipyridyl molecule in the asymmetric unit. In the case of (2A) the structure was obtained from THF in the triclinic space group $P\bar{1}$ with four molecules of (2) and two molecules of (A) in the asymmetric unit (Fig. 2).

In all three co-crystal structures identified containing (A), each of the N atoms on (A) forms a hydrogen bond to the OH group of the carboxylic acid group on the cinnamic acid derivative (Fig. 3) alongside weak π–π contacts (Tables 3, 4, S1, and Fig. S1 of the supporting information). In both (1A)
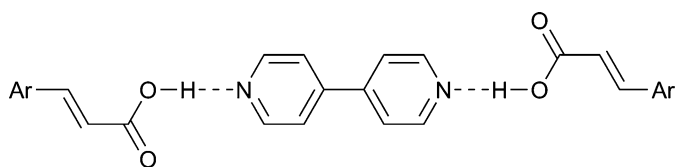
Figure 3
Illustration of the hydrogen-bonding interactions in co-crystals containing (A).

and (3A) the asymmetric unit contains half a molecule of (A), the other half of which is generated by an inversion centre, consequently the pyridyl rings of (A) are planar. In the case of (2A) the two unique molecules of (A) are twisted with torsion angles of −28.2 (2) (C57—C56—C53—C52) and 25.5 (2)° (C44—C43—C46—C50) between the pyridyl rings.

Examining the fingerprint plots associated with the Hirshfeld surfaces for each of the three structures shows consistent
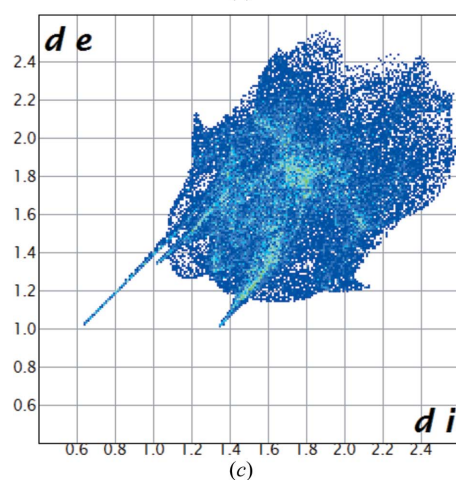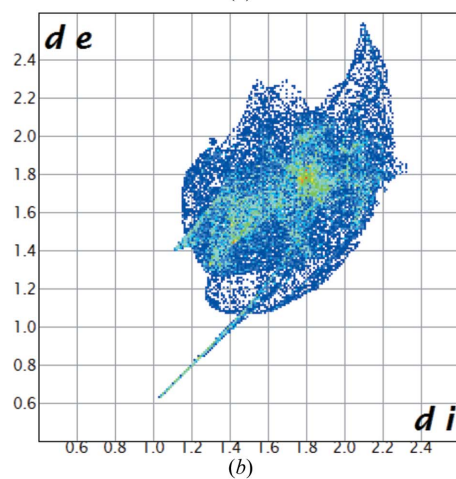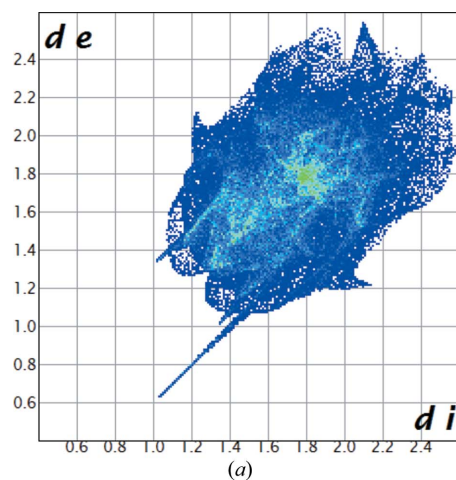

Figure 4
(1A) Fingerprint plots (a) dipyridyl and *trans*-cinnamic acid combined, (b) dipyridyl in the co-crystal, (c) *trans*-cinnamic acid in the co-crystal.

features as would be expected from their similar structures and consequently only those for (1A) are shown in Fig. 4. The O—H⋯N hydrogen bonding is depicted by the sharp pointed features *de* 0.6 Å, *di* 1.0 Å in Figs. 4(*a*) and (*b*), and *de* 1.0 Å, *di* 0.6 Å in Fig. 4(*c*). The other feature of note is the short C—H⋯O contacts highlighted by the short sharp spike at *de* 1.3 Å, *di* 1.0 Å in Figs. 4(*a*) and (*b*), and *de* 1.3 Å, *di* 1.0 Å in Fig. 4(*c*).

3.3. *Iso*-nicotinamide (*B*)

Co-crystals of (1B) and (3B) were crystallized from ethanol and THF, respectively, in the triclinic space group $P\bar{1}$ with two molecules of cinnamic acid derivative [*trans*-cinnamic acid in (1B) and 4-methoxycinnamic acid in (3B)] and two molecules of (B) in the asymmetric unit. The structure of (1B) has been previously reported (Aakeröy *et al.*, 2002). Co-crystals of (2B)

and (4B) crystallized from THF, in the case of (2B) in the triclinic space group $P\bar{1}$, while (4B) crystallized in the monoclinic space group $P2_1/c$. Both structures contained one molecule of the cinnamic acid derivative [4-methyl cinnamic acid for (2B) and 3,4-methoxycinnamic acid for (4B)] and one molecule of (B) in the asymmetric unit (Fig. 5).
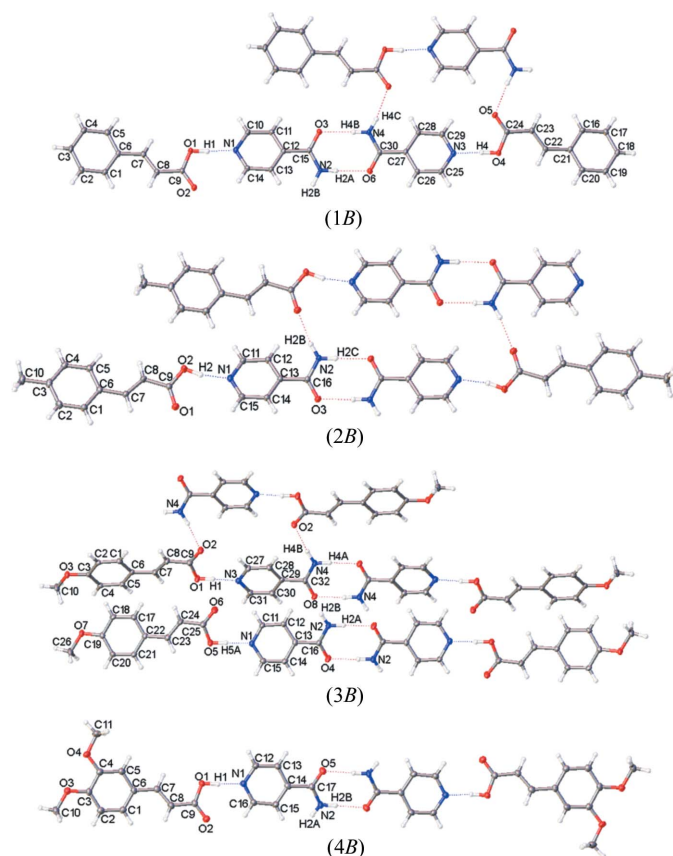

Figure 5
Structure of (1B), (2B), (3B) and (4B) with ellipsoids depicted at the 50% level. Hydrogen bonding is illustrated and the atom labelling shown.
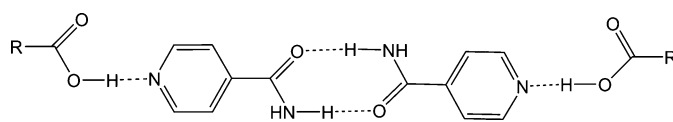

Figure 6
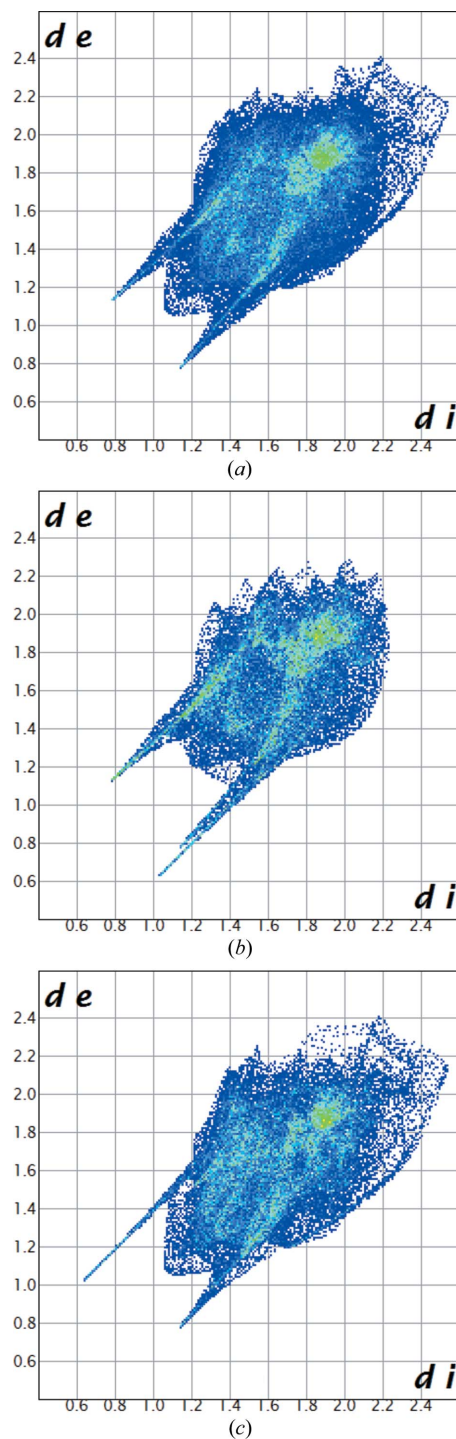Illustration of the hydrogen-bonding interactions in co-crystals containing (B).

Figure 7
(1B) Fingerprint plots (*a*) *iso*-nicotinamide and *trans*-cinnamic acid combined, (*b*) *iso*-nicotinamide in the co-crystal, (*c*) *trans*-cinnamic acid in the co-crystal.

In line with a previous study into the co-crystals of cinnamic acids and (*B*), during which the structure of (1*B*) was published (Aakeröy *et al.*, 2002), the three novel structures reported here [(2*B*), (3*B*) and (4*B*)] all contain carboxylic acid⋯pyridine (O—H⋯N) and amide⋯amide hydrogen-bonding interactions. This creates a hydrogen-bonded chain of four molecules terminated by cinnamic acid molecules which sandwich two molecules of (*B*), see Fig. 6, Tables 3 and S1.

Three of the structures [(1*B*), (2*B*) and (3*B*)] also displayed additional hydrogen-bonding interactions between the chains, with the O of the carboxylic acid and an amide NH, creating a four molecule wide offset ribbon through the structure (Fig. 6). In the fourth structure, the (4*B*) units are twisted with respect to each other, possibly due to the bulk created by the presence of two OMe substituents. In three of the structures weak π–π contacts were also identified (Table 4, Fig. S2), the exception was in (3*B*).

For all four of the structures, the Hirshfeld fingerprint plots show very similar features and hence only those for (1*B*) are illustrated in Fig. 7. The sharp features at $de \simeq 1.1$ Å, $di \simeq 0.8$ Å in Figs. 7(*a*) and (*b*) and $de \simeq 0.8$ Å, $di \simeq 1.1$ Å in Fig. 7(*c*), are due to the amide NH⋯O hydrogen-bond interactions, while the sharp features at $de \simeq 0.8$ Å, $di \simeq 1.1$ Å in Figs. 7(*a*) and (*b*), and $de \simeq 1.1$ Å, $di \simeq 0.8$ Å are associated with the carboxylic acid OH⋯N hydrogen bonds and the amide NH⋯O hydrogen-bond interaction. The apron around $de \simeq 1.1$ Å, $di \simeq 1.1$ Å are due to short H⋯H contacts.

3.4. Nicotinamide (*C*)

(1*C*) was crystallized from 2-propanol in the monoclinic space group $P2_1/c$ with one *trans*-cinnamic acid molecule and one nicotinamide in the asymmetric unit, Fig. 8. The amide group of the nicotinamide is twisted out of the plane of the pyridine with a torsion angle of -27.5 (2)° (C12—C13—C15—N2), while a torsion angle of -166.6 (2)° (C7—C8—C9—O1) is observed for the carboxylic acid. As with (1*B*) the structure contains hydrogen bonding between the carboxylic OH and the pyridine N, amide–amide hydrogen bonding and hydrogen bonding between the O of the carboxylic acid group and the amide NH (Table 3 and S1). Due to the non-planar orientation of the molecules, hydrogen bonding creates a three-dimen-
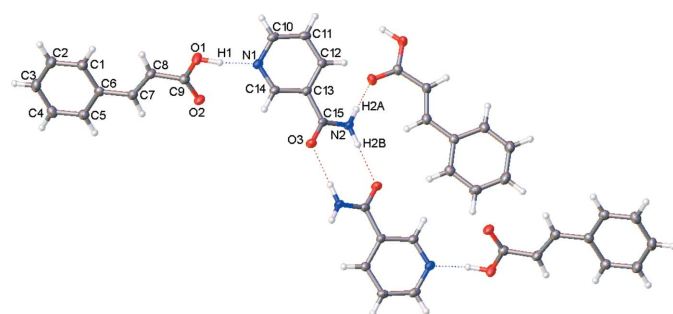
sional network. In addition π–π stacking contacts are observed (Table 4).

The Hirshfeld fingerprint plots for (1*C*) show the expected interactions. The sharp peak at $de \simeq 0.6$ Å, $di \simeq 1.0$ Å in Fig. 9(*b*) and $de \simeq 1.0$ Å, $di \simeq 0.6$ Å on Fig. 9(*c*) corresponds to the OH⋯N interactions. There is also a sharp peak at $de \simeq 1.1$ Å, $di \simeq 0.8$ Å in Figs. 9(*a*) and (*b*) corresponding to the OH⋯N
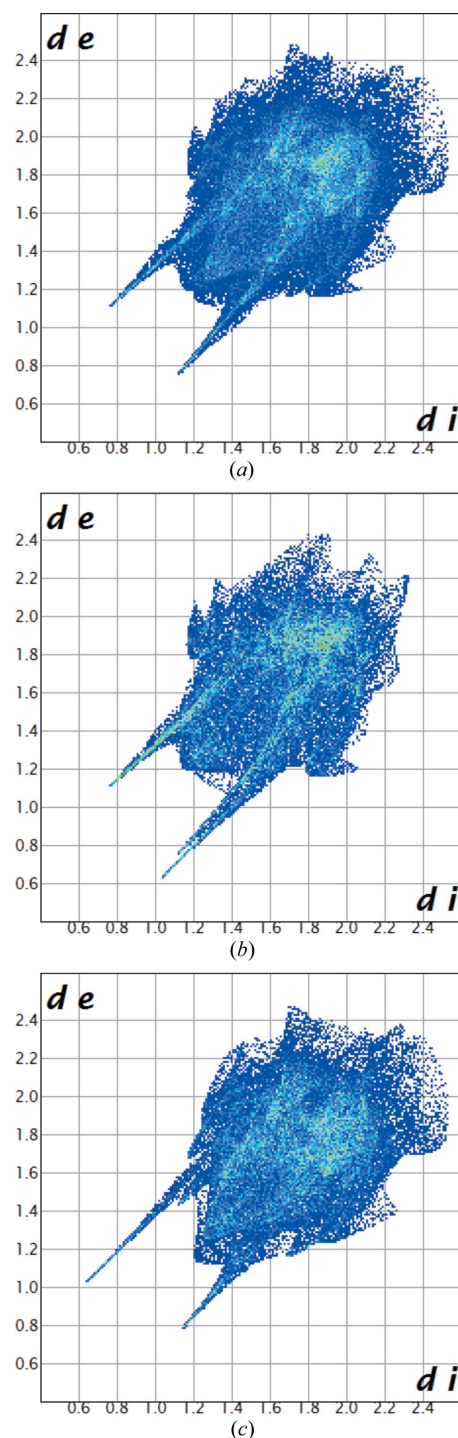

Figure 9
(1*C*) Fingerprint plots (*a*) nicotinamide and *trans*-cinnamic acid combined, (*b*) nicotinamide in the co-crystal, (*c*) *trans*-cinnamic acid in the co-crystal.

Figure 8
Structure of (1*C*) with ellipsoids depicted at the 50% level. Hydrogen bonding is illustrated and the atom labelling shown.

amide–amide hydrogen bonding. The sharp peak at $de \simeq$ 0.8 Å, $di \simeq 1.1$ Å in Figs. 9(a) and (c) relates to either the amide carboxylic NH$\cdots$O or the C10—H10$\cdots$O2 interactions.

3.5. Solvent drop ball mill grinding

The X-ray powder diffraction patterns of mixtures of cinnamic acid with a co-crystallizer after solvent drop grinding were compared with those of the reactants. The formation of a co-crystal was inferred by the absence of peaks corresponding to the reactants and the appearance of new peaks (see Figs. S4–S15). The presence of ethanol served to act as a catalyst in the successful formation of ten co-crystals, Table 2. None of the samples showed evidence of having formed a co-crystal following ball mill grinding under the same conditions in the absence of a small amount of ethanol. The only combinations which did not form co-crystals under the conditions employed here were those of 3,4-methoxycinnamic acid (4) with *iso*-nicotinamide (*B*) or nicotinamide (*C*). Powder patterns were simulated using *PowderCell*, Version 2.4 (Kraus & Nolze, 1996) from the eight crystal structures obtained herein and compared with the experimental powder patterns from the solvent drop grinding. There was generally good agreement between the experimental and simulated patterns for (1*A*), (1*B*), (1*C*), (2*A*), (2*B*), (3*A*) and (3*B*) apart from small shifts in the peak position due to the crystal structures having been obtained at 100 K and the powder patterns recorded at room temperature. The only peaks in experimental patterns for (4*B*) and (4*C*) are attributable to their two respective starting components.

4. Conclusions

A number of co-crystals of cinnamic acid derivatives, *trans*-cinnamic acid (1), 4-methylcinnamic acid (2), 4-methoxy cinnamic acid (3) and 3,4-methoxy cinnamic acid (4), with co-crystallizers, dipyridyl (*A*), *iso*-nicotinamide (*B*) and nicotinamide (*C*), were successfully synthesized by two different methods – recrystallization or solvent drop grinding. The solvent drop grinding resulted in ten co-crystals being obtained.

Single-crystal X-ray structures are reported for seven novel co-crystals of cinnamic acid derivatives with co-crystallizers. In the current study, single-crystal structures were not obtained for (2*C*), (3*C*) and (4*A*), although their formation was implied by powder X-ray diffraction after the respective components were combined by solvent drop ball milling. The predicted product (4*C*) was not formed under any of the preparation conditions tested. Further, more extensive attempts to form co-crystals of (4*C*) under different crystallization conditions may yield success in the future. In the case of the co-crystal structures reported here, the structures are strongly influenced by structure of the co-crystallizer rather than the cinnamic acid. This is perhaps not a surprise given that the cinnamic acid derivatives selected have relatively similar structures. In the two sets of cinnamic acid co-crystals formed with either dipyridyl or *iso*-nicotinamide, there are key hydrogen-bonding motif features that are observed for the specific co-crystallizer, and distinctive Hirshfeld fingerprint plots. In the case of the dipyridyl co-crystals, hydrogen-bonding interactions are formed between the OH group on the carboxylic acid and the pyridyl N, resulting in two cinnamic acid molecules per dipyridyl. The cinnamic acid derivative:*iso*-nicotinamide co-crystals formed in a 1:1 ratio and in-line with other cinnamic acid derivative:*iso*-nicotinamide co-crystal structures previously reported (Aakeröy *et al.*, 2002): hydrogen-bonding interactions were observed between the carboxylic acid OH and the N of the pyridyl, alongside amide–amide hydrogen-bonding interactions. No conclusions can be drawn about trends for cinnamic acid:nicotinamide co-crystals as only one 1:1 co-crystal (1*C*) was formed in the current study. The co-crystal structure of (1*C*) contained the same hydrogen-bonding interactions as those found for the cinnamic acid:*iso*-nicotinamide co-crystals. As noted in §1 the few examples of hydrates of cinnamic acid derivative co-crystals with *iso*-nicotinamide or nicotinamide have resulted in the formation of different hydrogen-bonding motifs to those observed here (Clarke *et al.*, 2010; Bevill *et al.*, 2014). In all of the co-crystal structures reported there was no evidence to suggest that proton transfer occurred within the hydrogen bonds to form a salt, based on the fact that the $X-D$ bond lengths were consistent with expected values and H atoms were located in the difference map within expected $D-H$ bonding distances.

References

Aakeröy, C. B., Chopade, P. D., Ganser, C., Rajbanshi, A. & Desper, J. (2012). *CrystEngComm*, **14**, 5845–5853.
Aakeröy, C. B. (1997). *Acta Cryst.* B**53**, 569–586.
Aakeröy, C. B., Beatty, A. M. & Helfrich, B. A. (2002). *J. Am. Chem. Soc.* **124**, 14425–14432.
Aakeröy, C. B., Fasulo, M. E. & Desper, J. (2007). *Mol. Pharm.* **4**, 317–322.
Aitipamula, S. *et al.* (2012). *Cryst. Growth Des.* **12**, 2147–2152.
Allen, F. H., Mahon, M. F., Raithby, P. R., Shields, G. P. & Sparkes, H. A. (2005). *New J. Chem.* **29**, 182–187.
Allen, F. H., Motherwell, W. D. S., Raithby, P. R., Shields, G. P. & Taylor, R. (1999). *New J. Chem.* **23**, 25–34.
Allen, F. H., Shields, G. P., Taylor, R., Allen, F. H., Raithby, P. R., Shields, G. P. & Taylor, R. (1998). *Chem. Commun.* pp. 1043–1044.
Bevill, M. J., Vlahova, P. I. & Smit, J. P. (2014). *Cryst. Growth Des.* **14**, 1438–1448.
Braga, D., Maini, L. & Grepioni, F. (2013). *Chem. Soc. Rev.* **42**, 7638–7648.
Brittain, H. G. (2012). *Cryst. Growth Des.* **12**, 5823–5832.
Bruker (2001). *SADABS*, Version 2012.1. Bruker AXS Inc., Madison, Wisconsin, USA.
Bučar, D.-K., Henry, R. F., Zhang, G. G. Z. & MacGillivray, L. R. (2014). *Cryst. Growth Des.* **14**, 5318–5328.
Clarke, H. D., Arora, K. K., Bass, H., Kavuru, P., Ong, T. T., Pujari, T., Wojtas, L. & Zaworotko, M. J. (2010). *Cryst. Growth Des.* **10**, 2152–2167.
Dolomanov, O. V., Bourhis, L. J., Gildea, R. J., Howard, J. A. K. & Puschmann, H. (2009). *J. Appl. Cryst.* **42**, 339–341.

Elder, D. P., Holm, R. & de Diego, H. L. (2013). *Int. J. Pharm.* **453**, 88–100.

Hemamalini, M., Loh, W.-S., Quah, C. K. & Fun, H.-K. (2014). *Chem. Cent. J.* **8**, 31.

Howard, J. A. K., Mahon, M. F., Raithby, P. R. & Sparkes, H. A. (2009). *Acta Cryst.* B**65**, 230–237.

James, S. L. *et al.* (2012). *Chem. Soc. Rev.* **41**, 413–447.

Jones, J. T. A., Hasell, T., Wu, X., Bacsa, J., Jelfs, K. E., Schmidtmann, M., Chong, S. Y., Adams, D. J., Trewin, A., Schiffman, F., Cora, F., Slater, B., Steiner, A., Day, G. M. & Cooper, A. I. (2011). *Nature*, **474**, 367–371.

Kraus, W. & Nolze, G. (1996). *J. Appl. Cryst.* **29**, 301–303.

Mahon, M. F., Raithby, P. R. & Sparkes, H. A. (2008). *CrystEngComm*, **10**, 573–576.

Moragues-Bartolome, A. M., Jones, W. & Cruz-Cabeza, A. J. (2012). *CrystEngComm*, **14**, 2552–2559.

Palatinus, L. & Chapuis, G. (2007). *J. Appl. Cryst.* **40**, 786–790.

Palatinus, L., Prathapa, S. J. & van Smaalen, S. (2012). *J. Appl. Cryst.* **45**, 575–580.

Palatinus, L. & van der Lee, A. (2008). *J. Appl. Cryst.* **41**, 975–984.

Seaton, C. C. (2011). *CrystEngComm*, **13**, 6583–6592.

Sheldrick, G. M. (2015). *Acta Cryst.* C**71**, 3–8.

Steed, J. W. (2013). *Trends Pharmacol. Sci.* **34**, 185–193.

Yates, J. L. R. & Sparkes, H. A. (2013). *CrystEngComm*, **15**, 3547–3553.

Zhu, W., Yi, Y., Zhen, Y. & Hu, W. (2015). *Small*, **11**, 2150–2156.

Zhu, W., Zhen, Y., Dong, H., Fu, H. & Hu, W. (2014). *Prog. Chem.* **26**, 1292–1306.